Structure of nanocrystalline GaN from X-ray diffraction, Rietveld and atomic pair distribution function analyses

V. Petkov,*[a] M. Gateshki,[a] J. Choi,[b] E. G. Gillan[b] and Y. Ren[c]

Received 6th July 2005, Accepted 30th August 2005
First published as an Advance Article on the web 23rd September 2005
DOI: 10.1039/b509577h

The three-dimensional structure of nanocrystalline GaN has been studied by X-ray diffraction, Rietveld and atomic pair distribution function (PDF) analyses. The material is of very limited structural coherence, yet possess a well-defined atomic arrangement resembling the wurtzite structure. The study demonstrates the great power of X-ray diffraction and the PDF approach in determining the three-dimensional structure of nanocrystalline materials.

1. Introduction

Crystalline GaN is a "III–V" compound with a very wide band-gap of 3.4 eV.[1] This semiconductor material has a high melting point, a high thermal conductivity, a large bulk modulus and a high breakdown voltage.[2] The material is used in commercially available applications such as short-wavelength light-emitting diodes and high power, high frequency transistors.[3] The useful properties of GaN have long been recognized in industry. However, the same properties making GaN a valuable semiconductor also make it extremely difficult to manufacture in bulk format suitable for wider industry applications. The difficulty is that large GaN crystals are not readily grown by high-temperature synthetic methods[4] due to the thermal instability of the material leading to its decomposition before melting ($T_m \sim$ 1500 °C). As a result, GaN semiconductors are mostly produced and used as thin films. Conventionally, GaN thin films are grown by chemical vapor deposition near 1000 °C.[5]

An alternative approach to producing GaN films and bulk solids is to use single-source precursor decomposition or soft synthetic routes conducted at temperatures well below 1000 °C. Selected examples include the solid-state pyrolysis of polymeric gallium amides[6] and the reaction of gallium and gallium amides in supercritical NH_3,[7] respectively. This approach usually yields very fine powders or nanoparticles that can grow into much larger crystallites upon subsequent annealing. The quality of thus obtained crystalline GaN depends very much on the structural characteristics of the fine powders. A good knowledge of those characteristics is obviously necessary to improve the efficiency of the alternative approaches for producing crystalline GaN. Usually the structure of materials is determined from the Bragg peaks in their diffraction patterns. However, fine powders lack the extended structural coherence of usual crystals and show diffraction patterns with a pronounced diffuse component and a few broad Bragg-like features. This renders the traditional diffraction techniques for structure determination very difficult to apply.

Recently, it has been shown that the three-dimensional (3D) structure of materials with reduced structural coherence, including nanoparticles, can be determined using the so-called atomic pair distribution function (PDF) analysis.[8–11] Here we employ Rietveld and PDF analyses to determine the 3D structure of nanocrystalline GaN powders obtained by low-temperature synthesis. We find that the nanopowders possess a well-defined atomic arrangement that may be described in terms of a locally disordered wurtzite structure.

2. Experimental

2.1 Sample preparation

Fine GaN powders were obtained through a low-temperature reaction between gallium chloride, $GaCl_3$, and sodium azide, NaN_3. Two reaction routes were employed: one involving a non-aqueous solvent and the other was solvent-free. The first reaction route is a solution reaction between gallium chloride and sodium azide to an insoluble azide precursor that decomposes solvothermally to GaN in superheated toluene at 260 °C.[12] The second route is a straightforward exchange reaction between gallium chloride and sodium azide producing GaN below 210 °C.[13] The as-synthesized solids were rigorously washed with glycerol–ethanol and ethanol or methanol to remove all NaCl by-products. Both reactions yield thermally stable GaN powders consisting of particles with an average size of 10 nm with various levels of aggregation as revealed by TEM experiments (see Fig. 1). In this respect the GaN powders studied by us are nanocrystalline in nature. Crystalline wurtzite GaN obtained from Aldrich was also studied and used as a reference sample. All three samples, crystalline GaN and GaN nanoparticles obtained in toluene and in a solvent-free environment, were carefully packed between Kapton foils and subject to synchrotron radiation scattering experiments.

2.2 Synchrotron radiation scattering experiments

Synchrotron radiation scattering experiments were carried out at the beamline 11-ID-C (Advanced Photon Source, Argonne National Laboratory) using X-rays of energy 115.232 keV (λ = 0.1076 Å). A Si standard was used to cross-check the X-ray energy calibration and beam line optics alignment. X-Rays of

[a]*Department of Physics, Central Michigan University, Mt. Pleasant, MI 48859, USA. E-mail: petkov@phy.cmich.edu*
[b]*Department of Chemistry, University of Iowa, Iowa City, IA-52242, USA*
[c]*Advanced Photon Source, Argonne National Laboratory, Argonne, Illinois 60439, USA*

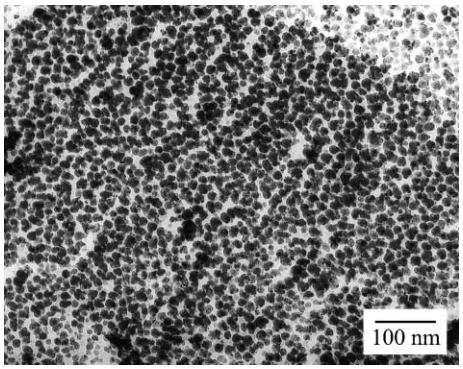

Fig. 1 TEM image of nanocrystalline GaN.

higher energy were used to obtain diffraction data to higher values of the wave vector, Q, which is important for the success of PDF analysis. The measurements were carried out in symmetric transmission geometry and scattered radiation was collected with an imaging plate detector (mar345). The use of an imaging plate detector greatly reduces the data collection time and improves the statistical accuracy of the diffraction data as demonstrated by recent experiments on materials with reduced structural coherence.[14] Five images were taken for each of the samples. The exposure time was 10 s per image. The corresponding images were combined, subjected to geometrical corrections, integrated and reduced to one dimensional X-ray diffraction (XRD) patterns using the computer program FIT2D.[15] Thus obtained XRD patterns for the three samples studied are shown in Figs. 2 and 3.

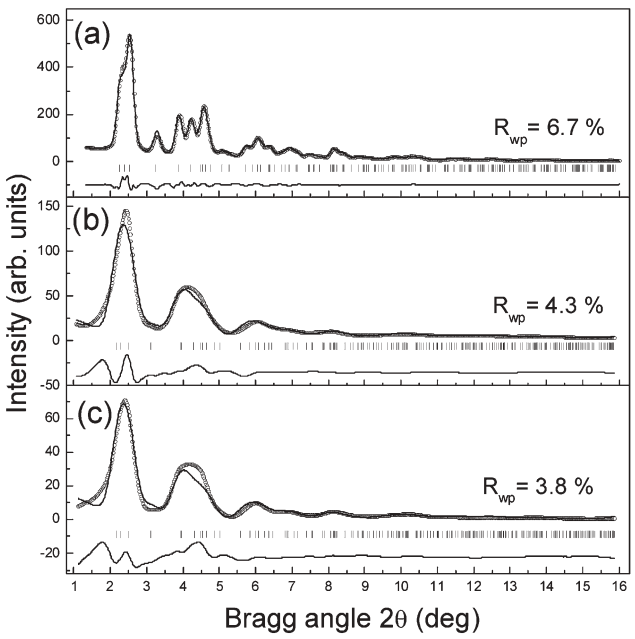

Fig. 2 Experimental XRD patterns (symbols) for crystalline GaN (a) and two nanocrystalline GaN samples obtained in a solvent free environment (b) and in toluene (c). Patterns calculated through a Rietveld refinement based on the wurtzite (hexagonal) structure are given as solid lines. The residual difference between the experimental and calculated data is given in the lower part of the plots. The positions of the Bragg peaks of the hexagonal structure are given as bars in the lower part of the plot. The agreement factors R_w are reported for each of the refinements.

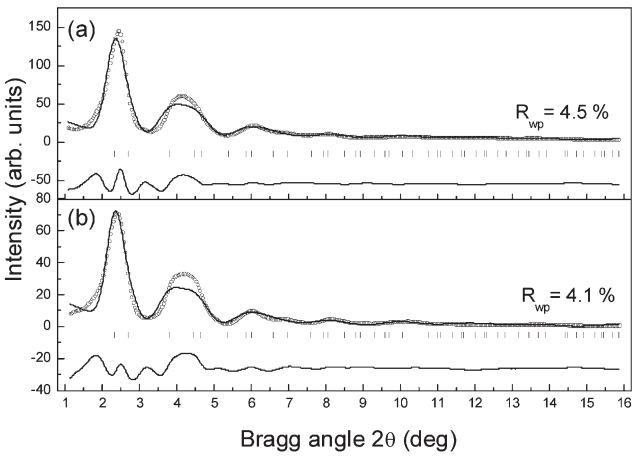

Fig. 3 Experimental XRD patterns (symbols) for two nanocrystalline GaN samples obtained in a solvent free environment (a) and in toluene (b). Patterns calculated through a Rietveld refinement based on the zinc-blende (cubic) structure are given as solid lines. The residual difference between the experimental and calculated data is given in the lower part of the plots. The positions of the Bragg peaks of the cubic structure are given as bars in the lower part of the plot. The agreement factors R_w are reported for each of the refinements.

3. Results

As can be seen in Fig. 2 the experimental XRD pattern of crystalline GaN exhibits well-defined Bragg peaks that could be indexed in a hexagonal unit cell with parameters $a = b =$ 3.18 Å and $c = 5.18$ Å. The material is obviously a 3D ordered and periodic solid. The diffraction patterns of the nanocrystalline samples shows only a few broad, Bragg-like peaks that merge into a slowly oscillating diffuse component already at Bragg angles as low as 8°. As our subsequent analyses show (see Figs. 2 and 3) these diffuse diffraction peaks can almost equally well be explained in terms of a hexagonal or cubic structure. Such diffraction patterns are typical for materials of very limited structural coherence, and are obviously difficult to be tackled by traditional techniques for structure determination. However, when reduced to the corresponding atomic PDFs, they become a structure-sensitive quantity lending itself to structure determination.

The frequently used atomic pair distribution function, $G(r)$, is defined as follows:

$$G(r) = 4\pi r[\rho(r) - \rho_0] \quad (1)$$

where $\rho(r)$ and ρ_0 are the local and average atomic number densities, respectively, and r is the radial distance. It peaks at characteristic distances separating pairs of atoms and thus reflects the atomic-scale structure. The PDF $G(r)$ is the Fourier transform of the experimentally observable total structure function, $S(Q)$, *i.e.*,

$$G(r) = (2/\pi) \int_{Q=0}^{Q_{max}} Q[S(Q) - 1] \sin(Qr) \mathrm{d}Q \quad (2)$$

where Q is the magnitude of the wave vector ($Q = 4\pi\sin\theta/\lambda$), 2θ is the angle between the incoming and outgoing radiation beams and λ is the wavelength of the radiation used. The structure function is related to the coherent part of the total scattered intensity as follows:

$$S(Q) = 1 + [I^{\mathrm{coh}}(Q) - \Sigma c_i|f_i(Q)|^2]/|\Sigma c_i f_i(Q)|^2 \qquad (3)$$

where $I^{\mathrm{coh}}(Q)$ is the coherent scattering intensity per atom in electron units and c_i and f_i are the atomic concentration and X-ray scattering factor, respectively, for the atomic species of type i.[16] As can be seen from eqns. (1–3), the PDF is simply another representation of the powder XRD data. However, exploring the diffraction data in real space is advantageous, especially in the case of materials of limited structural coherence. First, as eqns. (2) and (3) imply the *total* scattering, including Bragg scattering as well as diffuse scattering, contributes to the PDF. In this way both the average, longer-range atomic structure, manifested in the Bragg peaks, and the local structural imperfections, manifested in the diffuse component of the diffraction pattern, are reflected in the PDF. And second, the atomic PDFs do not imply any periodicity and can be used to study the atomic ordering in materials showing any degree of structural coherence, ranging from crystals[17] to glasses[18] and even liquids.[19] Recently, the atomic PDF approach has been successfully applied to nanocrystalline materials,[20–22] including nanoparticles.[23]

Experimental PDFs for the samples studied were obtained as follows. First, the coherently scattered intensities were extracted from the corresponding XRD patterns by applying appropriate corrections for flux, background, Compton scattering and sample absorption. The intensities were normalized in absolute electron units, reduced to structure functions $Q[S(Q) - 1]$ and Fourier transformed to atomic PDFs. Thus obtained experimental atomic PDFs are shown in Fig. 4. All data processing was done with the help of the program RAD.[24] As can be seen in Fig. 4, the experimental PDF for crystalline GaN is rich in well-defined structural features extending to high real-space distances, as it should be with a material possessing a perfect long-range atomic order. The PDFs for nanocrystalline GaN are also rich in structural features but they vanish at much shorter interatomic distances. This observation shows that nanocrystalline GaN, as one may expect, lacks the extended order of usual crystals. The first peak in the experimental PDFs shown in Fig. 4 is positioned at approximately 1.94(1) Å which is the average Ga–N first neighbor distance. The area under the peak yields four nitrogen neighbors for each gallium atom or, alternatively, four gallium neighbors for each nitrogen. The peak appears with the same shape and area in the PDFs for crystalline and nanocrystalline GaN (see the inset in Fig. 4) showing that they share the same immediate atomic order, that of fourfold coordinated Ga and N atoms. The second peak is positioned at approximately 3.16(2) Å. It reflects mostly the first neighbor Ga–Ga and, to a lesser extent, N–N distances due to the lower scattering power of the latter for X-rays. A careful inspection of that peak (see the inset in Fig. 4) shows that the distribution of Ga–Ga and N–N first neighbor distances in nanocrystalline GaN is much broader than that in GaN crystal. This indicates

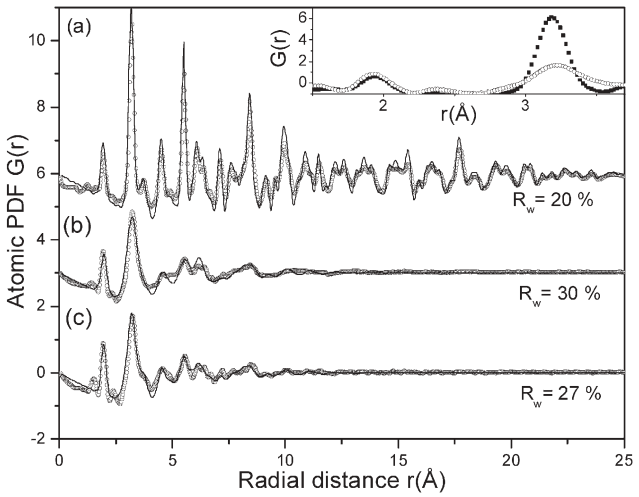

Fig. 4 Experimental (symbols) and model (solid line) PDFs for crystalline GaN (a) and two nanocrystalline GaN samples obtained in a solvent-free environment (b) and in toluene (c). The model PDFs are based on the wurtzite (hexagonal) structure. The agreement factors R_{w} are reported for each of the refinements. The first two peaks in the experimental PDFs for crystalline (■) and nanocrystalline (○) GaN are given in the inset on an enlarged scale.

that GaN nanopowders not only lack the extended order of usual crystals but also exhibit a considerable local structural disorder substantially disturbing their next nearest and more distant atomic arrangement. Moreover, a closer look at the experimental PDFs for the nanocrystalline samples shows that they decay almost to zero at interatomic distances ($\sim$1 nm) much shorter than the average nanoparticle's size ($\sim$10 nm; see Fig. 1). This observation shows that the local structural disorder and not the nanoparticle's size is the factor limiting the structural coherence in the nanopowders studied by us.

4. Discussion

To reveal the 3D structure of nanocrystalline GaN we approached the experimental XRD patterns with the widely employed Rietveld analysis first. Rietveld analysis[25] is a well-established technique for crystal structure determination and refinement from powder diffraction data. The method employs a least-squares procedure to compare experimental Bragg intensities with such calculated from a plausible structural model. The parameters of the model are then adjusted until the best fit to the experimental diffraction data is achieved. The progress of the fit is assessed by computing various agreement factors with the most frequently used being[26]

$$R_{\mathrm{w}} = \left\{ \frac{\sum w_i \left(y_i^{\mathrm{obs}} - y_i^{\mathrm{calc}}\right)^2}{\sum w_i \left(y_i^{\mathrm{obs}}\right)^2} \right\}^{\frac{1}{2}} \qquad (4)$$

where y_i^{obs} and y_i^{calc} are the observed and calculated data points and w_i are weighting factors taking into account the statistical accuracy of the diffraction experiment. The Rietveld analyses were carried out with the help of the program FullProf.[27] The XRD pattern for crystalline GaN was used as a reference and also analyzed with the Rietveld technique.

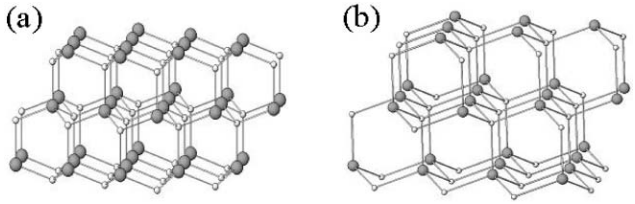

Fig. 5 Fragments from the (a) wurtzite ($P6_3mc$) and (b) zinc-blende ($F\bar{4}3m$) structures occurring with crystalline GaN.

GaN usually crystallizes in the wurtzite (hexagonal) structure[28] and it has been successfully grown in the zinc-blende (cubic) structure.[29] Fragments from the structures are shown in Fig. 5. As can be seen in the figure, each gallium and nitrogen is tetrahedrally coordinated in both structures. The next nearest and more distant coordination sequence is, however, very different in the two structures. Results from the Rietveld analysis of the experimental XRD patterns in terms of the wurtzite structure are shown in Fig. 2. Those in terms of the zinc-blende structure are shown in Fig. 3. The refined values of the parameters of the two structural models are summarized in Table 1 and 2, respectively. As can be seen in Fig. 2, the XRD pattern of crystalline GaN is perfectly reproduced by a model based on the wurtzite structure. The refined structural parameters agree very well with literature data.[28] The XRD patterns for the two nanocrystalline samples are almost equally well reproduced by the wurtzite and zinc-blende structure as a comparison between the data presented in Fig. 2 and 3 shows. Neither the values of the agreement factors R_w nor the residual difference between the computed and experimental XRD data allows one to draw a definitive conclusion in favor of either of the two substantially different structure types attempted. Moreover, the Rietveld analysis of the XRD data for the nanocrystalline samples yielded negative values for the mean-square atomic displacements (known as thermal factors, B; see Tables 1 and 2). Such unphysical results are often obtained with Rietveld analyses of powder diffraction patterns for materials with considerable structural disorder. The problems stems from the inability of the Rietveld analysis to properly handle diffraction patterns showing both broad Bragg peaks and pronounced diffuse scattering. As we demonstrate below, the difficulties are greatly reduced when the diffraction data are analyzed in terms of the corresponding atomic PDFs. Similarly to the Rietveld analysis, the PDF analysis employs a least-squares procedure to compare experimental and model data (PDF) calculated from a plausible structural model. The structural parameters of the model (unit cell constants, atomic coordinates and thermal factors) are adjusted until the best possible fit to the experimental data is achieved. The progress of the refinement is assessed by computing an agreement factor, R_w:

$$R_w = \left\{ \frac{\sum w_i \left(G_i^{exp} - G_i^{calc}\right)^2}{\sum w_i \left(G_i^{exp}\right)^2} \right\}^{1/2} \quad (5)$$

where G_i^{exp} and G_i^{calc} are the experimental and calculated PDFs, respectively, and w_i are weighting factors reflecting the statistical quality of the individual data points.

Results from the PDF analyses of the experimental data in terms of the wurtzite structure are presented in Fig. 4. The refined values of the structural parameters resulted from the analysis are summarized in Table 1. Results from the PDF analysis of the experimental data in terms of the zinc-blende structure are shown in Fig. 6. The analyses were done with the help of the program PDFFIT.[32] As can be seen in Fig. 4, the experimental PDF for crystalline GaN is very well reproduced by a model based on the wurtzite structure. A model based on the zinc-blende structure does not even come close to the

Table 1 Structural parameters for crystalline and nanocrystalline GaN obtained through Rietveld and PDF analyses. The structure is wurtzite (hexagonal, $P6_3mc$ space group) and Ga and N occupy Wyckoff positions 2b with fractional coordinates (1/3, 2/3, z). Atomic coordinates marked with an asterisk were not possible to refine. The agreement factors, R_w, are also reported for each of the refinements

	Crystalline GaN		GaN solvent-free		GaN in solvent	
	Rietveld	PDF	Rietveld	PDF	Rietveld	PDF
a,b/Å	3.181(3)	3.18(1)	3.143(4)	3.20(1)	3.142(4)	3.19(1)
c/Å	5.184(4)	5.18(1)	5.73(2)	5.28(2)	5.72(2)	5.28(2)
z(Ga)	0.000(2)	0.000(2)	0.000*	0.001(2)	0.000*	0.001(1)
z(N)	0.337(2)	0.336(2)	0.375*	0.336(2)	0.375*	0.376(2)
$B_{(Ga)}$/Å^2	0.40(2)	0.36(5)	−0.92(5)	0.80(5)	−0.98(2)	0.78(5)
$B_{[N]}$/Å^2	1.0(2)	0.85(5)	−0.5(2)	2.1(1)	−0.7(2)	2.3(1)
R_w	6.7%	20%	4.3%	30%	3.8%	27%

Table 2 Structural parameters for nanocrystalline GaN obtained through Rietveld refinement. The structure is zinc-blende (cubic, $F\bar{4}3m$ space group) and Ga and N occupy Wyckoff positions 4c (1/4, 1/4, 1/4) and 4a (0, 0, 0), respectively. The agreement factors, R_w, are also reported for each of the refinements

	GaN solvent-free	GaN in solvent
a/Å	4.598(4)	4.601(5)
$B_{(Ga)}$/Å^2	−0.92(5)	−0.95(5)
$B_{[N]}$/Å^2	0.1(2)	0.1(2)
R_w	4.5%	4.1%

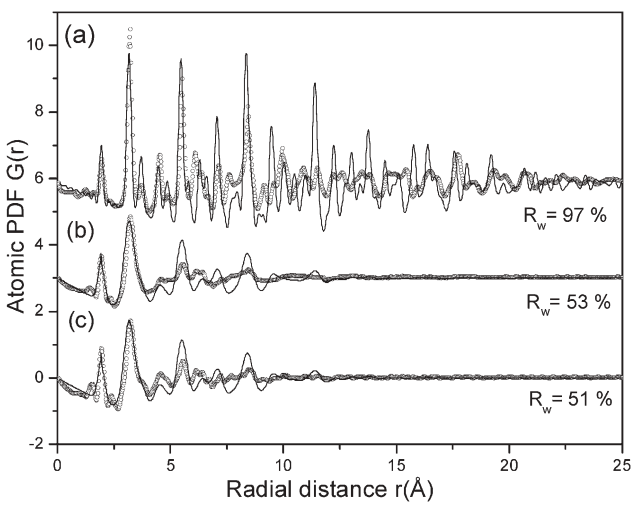

Fig. 6 Comparison between the experimental (symbols) and model (solid line) PDFs for crystalline GaN (a) and two nanocrystalline GaN samples obtained in a solvent free environment (b) and in toluene (c). The model PDFs are based on the zinc-blende (cubic) structure. The agreement factors R_w are reported for each of the comparisons.

experimental data as the result presented in Fig. 6 show. Also, the wurtzite-based fit yields structural parameters that are in very good agreement with the present Rietveld and previous results (see Table 1). The agreement well documents the fact that atomic PDFs truly reflect the atomic arrangement in materials and provides a reliable quantitative basis for structure determination. It may be noted that the agreement factor achieved with the PDF analysis (R_w = 20%) appears somewhat high when compared to the agreement factor R_{wp} of 6.7% resulted from the Rietveld analysis of the diffraction data in reciprocal space. This does not indicate an inferior structure refinement (compare the corresponding structural parameters in Table 1) but merely reflects the fact that the atomic PDF differs from the corresponding XRD pattern and is a quantity much more sensitive to the local atomic arrangement. As a result, R_w's greater than 20% are common with PDF analyses even of well-crystallized materials.[8,30,31] The inherently higher absolute value of the goodness-of-fit factors resulted from PDF analyses does not affect R_w's functional purpose as a residual function that must be minimized to find the best agreement between model and experimental data and as a quantity allowing to differentiate between competing structural models. It may also be noted that when the atomic pair correlation function, $g(r)$, defined as $g(r) = \rho(r)/\rho_0$, is used to guide a refinement of a structural model, the resulting agreement factors R_w are significantly lower than those reported from a refinement based on the corresponding PDF $G(r)$, and very close to the values of the agreement factors reported from Rietveld analyses. We, however, prefer to work with the PDF $G(r)$ and not $g(r)$, since the former scales with the radial distance r (see the multiplicative factor in the definition of $G(r)$; eqn. (1)) and is thus more sensitive to the longer-range atomic correlations.

As can be seen in Fig. 6, a model based on the zinc-blende structure is not capable of reproducing the experimental PDF data for nanocrystalline GaN. The lack of agreement between the model and the data is especially noticeable in the region of real space distances from 5 to 10 Å where the next nearest interatomic correlations in nanocrystalline GaN show up. On the other hand, a model based on the wurtzite structure (see Fig. 4) does a very good job in reproducing the PDF data. This result clearly demonstrates the ability of PDF technique to differentiate between competing structural models even in case of materials of very limited structural coherence. Moreover, as the data presented in Table 1 show, the PDF technique yields realistic values for the structural parameters of such materials, including the mean-square atomic displacements. In summary, the PDF analysis reveals the following details in the 3D structure of GaN nanosize powders: Both nanocrystalline samples studied have atomic arrangements that may very well be described in terms of a four atom hexagonal unit cell of the wurtzite type. In this respect our samples differ from other GaN fine powders that have been reported to be a mixture of cubic and hexagonal[6] or entirely cubic nanoparticles.[7] The wurtzite-type arrangement in GaN nanoparticles studied by us exhibits a considerable local structural disorder as the rather large mean-square atomic displacements indicate (compare the so-called thermal factors for crystalline and nanocrystalline GaN reported in Table 1). This disorder limits the structural coherence length to distances of 1–2 nm which is only a fraction of the average nanoparticle's size. Nevertheless the characteristic features of the wurtzite-type arrangement prevail and the nanoparticles are most likely to form hexagonal bulk GaN upon subsequent annealing as observed in practice.[12,13] From a practical point of view, given the great similarity between the 3D structure of the two nanocrystalline samples studied, one may concentrate on the more technologically efficient of the two routes employed here for producing fine GaN powders and further streamline it for larger-scale applications.

5. Conclusions

The atomic arrangement in nanocrystalline GaN has been studied by synchrotron radiation scattering experiments, Rietveld and atomic PDF analyses. The material is found to possess a well-defined atomic arrangement resembling a wurtzite-type structure with substantial local structural disorder. Although the structural coherence length in nanocrystalline GaN is reduced to only a few nanometres its structure may be described in terms of a four atom hexagonal unit cell.

The study is another demonstration of the ability of the PDF technique to yield three-dimensional structural information for materials of limited structural coherence, including nanoparticles. The technique succeeds because it relies on total scattering data obtained from the material and, as a result, is sensitive to its essential structural features regardless of crystalline periodicity and size. The PDF technique has the potential to become the highly needed tool for structure characterization in the rapidly growing field of engineering materials at the nanoscale.

Acknowledgements

Thanks are due to Mark Beno, Argonne National Laboratory for the help with the synchrotron experiments. This work was supported by the NSF through Grant DMR-0304391 NIRT (V. P.) and Grant CHE-0407753 (E. G. G.). The Advanced Photon Source is supported by DOE under contract W-31-109-Eng-38.

References

1 H. Morkoc, S. Strite, G. B. Gao, M. E. Lin, B. Sverdlov and M. Burns, *J. Appl. Phys.*, 1994, **76**, 1363–1398.
2 W. Martiessen, in *Condensed Matter and Materials Data*, ed. W. Martienssen and H. Warlimont, Springer, Berlin, 2005.
3 S. Nakamura, T. Mukai and M. Senoh, *Appl. Phys. Lett.*, 1994, **64**, 1687–1689.
4 J. Karpinski, J. Jun and S. Porowski, *J. Cryst. Growth*, 1984, **66**, 1–10.
5 S. Nakamura, T. Mukai, M. Senoh, S. Nagahama and N. Iwasa, *J. Appl. Phys.*, 1993, **74**, 3911–3915.
6 J.-W. Hwang, J. P. Campbell, J. Kozubowski, S. A. Hanson, J. F. Evans and W. L. Gladfelter, *Chem. Mater.*, 1995, **7**, 517–525.
7 A. P. Purdy, *Chem. Mater.*, 1999, **11**, 1648–1649.
8 V. Petkov, E. Bozin, S. J. L. Billinge, T. Vogt, P. Trikalitis and M. Kanatzidis, *J. Am. Chem. Soc.*, 2002, **124**, 10157–10162.
9 V. Petkov, S. J. L. Billinge, P. Larson, S. D. Mahanti, T. Vogt, K. K. Rangan and M. Kanatzidis, *Phys. Rev. B*, 2002, **65**, 092105–092109.

10 V. Petkov, P. Zavalij, S. Lutta, M. S. Whittingham, V. Parvanov and S. Shastri, *Phys. Rev. B*, 2004, **69**, 085410–085416.
11 M. Gateshki, S.-J. Hwang, D. H. Park, Y. Ren and V. Petkov, *J. Phys. Chem. B*, 2004, **108**, 14956–14963.
12 L. Grocholl, J. Wang and E. G. Gillan, *Chem. Mater.*, 2001, **13**, 4290–4296.
13 J. Wang, L. Grocholl and E. G. Gillan, *Nano Lett.*, 2002, **2**, 899–902.
14 (*a*) P. J. Chupas, X. Qiu, P. Lee, C. P. Grey and S. J. L. Billinge, *J. Appl. Crystallogr.*, 2003, **36**, 1342–1347; (*b*) V. Petkov, D. Qadir and S. D. Shastri, *Solid State Commun.*, 2004, **129**, 239–243.
15 A. P. Hammersley, M. Hanfland and D. Hausermann, *High Pressure Res.*, 1996, **14**, 235–248.
16 H. P. Klug and L. E. Alexander, *X-Ray Diffraction Procedures for Polycrystalline Materials*, Wiley, New York, 1974.
17 V. Petkov, I.-K. Jeong, J. S. Chung, M. F. Thorpe, S. Kycia and S. J. L. Billinge, *Phys. Rev. Lett.*, 1999, **83**, 4089–4093.
18 V. Petkov, S. J. L. Billinge, S. D. Sashtri and B. Himmel, *Phys. Rev. Lett.*, 2000, **85**, 3436–3439.
19 V. Petkov and G. Yunchov, *J. Phys.: Condens. Matter*, 1996, **8**, 6145–6156.
20 V. Petkov, S. J. L. Billinge, T. Vogt, A. S. Ichimura and J. L. Dye, *Phys. Rev. Lett.*, 2002, **89**, 0755021–0755024.
21 V. Petkov, S. J. L. Billinge, P. Larson, S. D. Mahanti, T. Vogt, K. K. Rangan and M. G. Kanatzidis, *Phys. Rev. B*, 2002, **65**, 092105–092109.
22 V. Petkov, P. Y. Zavalij, S. Lutta, M. S. Whittingham, V. Parvanov and S. D. Shastri, *Phys. Rev. B*, 2004, **69**, 085410–085416.
23 B. Gilbert, F. Huang, H. Z. Zhang, G. A. Waychunas and J. F. Banfield, *Science*, 2004, **305**, 651–654.
24 V. Petkov, *J. Appl. Crystallogr.*, 1989, **22**, 387–389.
25 H. M. Rietveld, *J. Appl. Crystallogr.*, 1969, **2**, 65–70.
26 R. A. Young, in *The Rietveld Method*, ed. R. A. Young, Oxford University Press, New York, 1996.
27 J. Rodríguez-Carvajal, *Physica B*, 1993, **192**, 55–58.
28 R. W. G. Wyckoff, in *Crystal Structures*, John Wiley & Sons, New York, 1963.
29 D. J. As, D. Schikora, A. Greiner, M. Lubbers, J. Mimkes and K. Lischka, *Phys. Rev. B*, 1996, **54**, R11118–R11121.
30 M. Gateshki, S.-J. Hwang, D. H. Park, Y. Ren and V. Petkov, *J. Phys. Chem. B*, 2004, **108**, 14956–14963.
31 V. Petkov, S. J. L. Billinge, J. Heising and M. G. Kanatzidis, *J. Am. Chem. Soc.*, 2000, **122**, 11572–11576.
32 Th. Proffen and S. J. L. Billinge, *J. Appl. Crystallogr.*, 1999, **32**, 572–575.